NASA Technical Memorandum 82691

# QCSEE Under-The-Wing Engine Acoustic Data




Harry E. Bloomer and Nick E. Samanich
*Lewis Research Center*
*Cleveland, Ohio*

May 1982

NASA

# QCSEE UNDER-THE-WING ENGINE ACOUSTIC DATA

Harry E. Bloomer and Nick E. Samanich

## SUMMARY

A major objective of the Quiet, Clean, Short-Haul, Experimental Engine (QCSEE) program was the development of very low-noise propulsion system technology. Both an over-the-wing (OTW) and an under-the-wing (UTW) experimental engine were designed and built under this program. The UTW engine had a variable-geometry fan exhaust nozzle and a variable-pitch fan that provided quick-response reverse thrust capability. An automatic digital control enabled optimal engine operation under all steady-state conditions as well as during forward and reverse thrust transient operation. The engine was tested at the Engine Noise Test Facility alone and with wing and flap segments to simulate an installation on a short-haul transport aircraft. The engine acoustic configuration was varied to give 14 test configurations. This report documents, in tabular form, all of the acoustic test results from the UTW program at Lewis. The results are presented as 1/3-octave-band sound pressure level (SPL) tabulations for all of the test points and some narrow- band spectra and 1/3-octave-band data plots for selected conditions.

## INTRODUCTION

As part of a broad-based NASA program to provide a technology base for future propulsion requirements for powered-lift aircraft, the Quiet, Clean, Short-Haul, Experimental Engine (QCSEE) program was begun by the Lewis Research Center in 1974 (refs. 1 and 2). A major objective of the program was the development of very low-noise propulsion system technology. The QCSEE engines were designed to meet very challenging noise goals. A 95-EPNdB noise goal on a 152-m (500-ft) sideline was established for powered-lift takeoff and approach on a 610-m (2000-ft) runway at the altitude at which maximum noise is produced (ref. 3). Both an over-the-wing (OTW) and an under-the-wing (UTW) experimental engine were designed and built under this program. The UTW design was reported in reference 4. The initial buildup of the UTW engine was tested by the contractor at his test site. Initial UTW acoustic test results were reported in reference 5. The UTW engine was inspected, refurbished, and delivered to the NASA Lewis Research Center in 1978 for further testing. Other results of QCSEE testing at Lewis were reported in references 3, 6, and 7.

The engine incorporated many low-noise design features, including a hybrid inlet, wide rotor-stator spacing, frame treatment and treated vanes, stacked treatment in the core to attenuate both turbine noise and low-frequency core noise, and treated, removable fan exhaust wall panels and splitter. Details of the acoustic design are contained in references 8 and 9.

The UTW engine had a variable-geometry fan exhaust nozzle and a variable-pitch fan that provided quick-response reverse thrust capability. An automatic digital control (ref. 10) enabled optimal engine operation under all steady-state conditions as well as during forward and reverse thrust transient operation.

The engine was tested at the Engine Noise Test Facility alone and with wing and flap segments to simulate an installation on a short-haul transport

aircraft. The engine acoustic configuration was varied to give 14 test configurations. The fan blade angle was varied from $+5.2^{o}$ to $-7.6^{o}$ and the exhaust nozzle area was varied from 1.52 to 1.87 $m^2$ (2350 to 2900 $in^2$) to simulate both approach and takeoff power conditions.

References 3 and 6 reported portions of the data obtained in the program. This report documents, in tabular form, all of the acoustic test results from the UTW program at Lewis. The results are presented as 1/3-octave-band sound pressure level (SPL) tabulations for all of the test points and as narrowband spectra and 1/3-octave-band data plots for some selected conditions. Although this report does not consider the deterministic modeling of the jet surface interaction noise sources for the QCSEE UTW powered-lift system, reference 11 presents QCSEE scale-model test data to which quasi-deterministic models have been applied and which therefore may be of interest to the reader.

## APPARATUS AND PROCEDURE

### UTW Experimental Propulsion System

The UTW experimental propulsion system, shown in figure 1, features a composite-structure, high-Mach-number (accelerating) inlet; a gear-driven, variable-pitch fan with composite fan blades; a composite fan frame; an acoustically treated fan duct with an acoustic splitter ring; a variable-geometry fan exhaust nozzle; an advanced (F-101) core and low-pressure turbine; an acoustically treated core exhaust nozzle; top-mounted engine accessories; and a digital electronic control system combined with a hydromechanical fuel control. The fundamental engine design criteria were influenced by the fan engine cycle required to meet total system noise objectives, which were dictated by jet-flap noise constraints.

The fan is a low-pressure-ratio (1.27), low-tip-speed (289.6 m/sec, 950 ft/sec) configuration sized to provide 405.5 kg/sec (894 lb/sec) of corrected airflow. The fan contains 18 composite, variable-pitch fan blades with flight-weight disks and blade supporting system. The fan is driven by the F-101 low-pressure turbine through a main reduction gear. The reduction gear is a six-star epicyclic configuration with a gear ratio of 2.465 and a takeoff power rating of 9806 kW (13 145 hp).

The fan is capable of blade pitch change from forward to reverse thrust through either flat pitch or stall pitch. Two variable-pitch fan actuation systems were developed for the UTW experimental engine. A cam/harmonic drive system was developed by the Hamilton Standard Division of United Technology Corp. under subcontract to the General Electric Co., and a ball spline actuation system was developed by GE. The rotary motion power required to drive both systems was provided by hydraulic motors. Both systems were designed to move the blades from their forward thrust position to reverse in less than 1 sec.

The fan frame is a flight-weight composite structure containing integral acoustic treatment, outer-casing blade containment, and fan tip treatment. The 33 integral outlet guide vanes also act as structural struts. The outer casing of the frame provides both inner and outer nacelle flow paths. A core inlet flow path and mounts for the forward bearings, gears, radial drive, etc, are also integrally provided.

The nacelle components include a lightweight composite hybrid inlet that provides acoustic suppression at takeoff power by means of a high throat Mach

number (0.79) and integral acoustic treatment. The composite fan duct, acoustic splitter, and core cowl are hinged from the pylon to provide access for engine maintenance. The core exhaust nozzle and nozzle plug are acoustically treated to reduce aft-radiated core noise. The fan exhaust nozzle is a variable-area, four-flap design capable of area change from takeoff to cruise, that can open to a flared position to form an inlet in the reverse thrust mode. The nozzle flaps are hydraulically actuated.

Engine fuel flow, blade pitch angle, and exhaust nozzle area are controlled by a digital electronic control. Major engine accessories are mounted on a boilerplate gearbox on top of the fan frame.

The UTW experimental propulsion system was designed to provide 81 400 N (18 300 lb) of uninstalled thrust and 77 400 N (17 400 lb) of installed thrust at takeoff on a 305.6 K (90° F) day.

## Engine Acoustic Design Features

Table I lists the acoustic design parameters of the engine. Table II lists "as tested" values of pertinent parameters.

Figure 2 summarizes the main acoustic features of the engine. A high inlet throat Mach number (0.79) is used to suppress inlet noise at takeoff. Wall treatment having a length equal to 0.74 fan diameter ($L_T/D_F = 0.74$) is added to provide suppression at approach and in reverse thrust. The rotor-stator combination has 1.5-tip-chord spacing and a vane-blade ratio (1.83) selected to reduce second harmonic noise due to rotor-stator interaction (ref. 4). Fan exhaust suppression utilizes inner and outer wall treatment with varying thicknesses to obtain increased suppression bandwidth. A treated 1-m (40-in.) splitter is necessary to obtain the required suppression level. A major concern in the aft duct is noise generated by flow over the treated surfaces, struts, and splitter. To keep these sources below the suppressed fan noise, the average duct Mach number is limited to 0.47. The core suppressor is a stacked design that has a combination of low-frequency absorption cells to reduce combustor noise and thinner treated panels on the inner and outer walls to reduce the high-frequency turbine noise. Treatment is also applied in the core inlet passage to reduce forward-radiated compressor noise. Schematics showing acoustic design details for the inlet, the fan exhaust duct, and the core exhaust are presented in figures 3(a), (b), and (c) respectively.

## Engine and Wing-Flap Configurations

The single-degree-of-freedom (SDOF) acoustic configurations embodying all of the design features shown in detail in figure 3 are shown schematically in figure 4 and tabulated in table III. Splitter-in fully suppressed configuration 1 and splitter-out configuration 2 are shown in the bottom and top halves of figure 4, respectively. The substitution of the bulk absorber treatment (see ref. 6 for more details), designated configuration 3, for the SDOF treatment in the fan duct is detailed in figure 5. The bulk absorber panels were constructed as follows: Structural channels were bonded to a solid back face. An advanced aramid fiber, Dupont Kevlar 29, which was treated to have low moisture absorption, was installed in the 2.5-cm (1-in.) deep cavities to a nominal bulk density of 56 kg/m$^3$ (3.5 lb/ft$^3$). A 0.075-cm (0.0295-in.) thick perforated faceplate was then bonded and riveted to the top of the structural channels. The perforated faceplate had 0.15-cm (0.059-in.) diam-

eter holes with an open area of about 30 percent. Taping the front half of the fan duct treatment yielded configuration 4. Complete taping of the fan duct and nozzle flaps yielded hard-wall configuration 5. The other acoustic treatment shown in figures 3(a) and (c) was also used in configurations 1 to 5. The baseline engine with bellmouth inlet, configuration 6, is shown in figure 6. It was untreated with the exception of the fan frame and vanes.

A variety of engine and wing configuration combinations were tested in the NASA UTW engine test program. The wing-flap segment used was a modified two-flap NASA supercritical airfoil design recommended by NASA Langley for short-haul aircraft as described in reference 12. The location of the engine relative to the wing-flap system was based on Langley data that indicated good powered-lift performance. No consideration was given, however, to acoustic optimization, although studies performed at Lewis (refs. 13 and 14) concluded that the dimensionless nozzle-to-flap separation distance X/D (where X is the distance from the fan exhaust exit plane to the wing flaps measured along the engine centerline, as shown in figure 7, and D is the engine fan exhaust nozzle maximum diameter) resulting from use of the QCSEE engine should produce reductions in jet-flap interaction noise. Engine wing-flap configurations (table III) included four different settings of the flap trailing-edge angle $\psi$, as shown in figure 7. Two takeoff settings with $\psi = 20^{0}$ (fig. 7(b), configurations 1B and 2B) and $\psi = 30^{0}$ (fig. 7(c) configurations 1C and 6C), an approach setting with $\psi = 60^{0}$, (fig. 7(d), configurations 1D, 2D*, 2D, 2D$^{+}$, and 6D), and a fully retracted "cruise" position (fig. 7(a), configuration 1A) were tested. The flap angles are measured from the main wing-segment chord centerline to the flap chord centerline. Dimensions of the engine and the wing and flap cross sections are also shown in figure 7. The separation distance ratio X/D was typically about 5 at takeoff and 4 at approach. The engine centerline was 4.57 m (15 ft) above ground level. The span of the vertically mounted wing-flap segment was 7.31 m (24 ft), with the upper edge 7.92 m (26 ft) above ground level. Table III lists the configurations tested.

## Facility and Microphone Systems

The test program was performed at the Engine Noise Test Facility located at the NASA Lewis Research Center. The facility is shown schematically in figure 8(a) and photographically in figure 8(b).

Two microphone systems were employed in the test program: a ground-plane system, and an overhead system. The 14 ground-plane microphones were positioned at $10^{0}$ increments at selected locations on a 45.7-m (150-ft) radius arc (fig. 8(a)). Microphones located within $10^{0}$ or $20^{0}$ of the deflected jet flow line during the engine and wing tests were severely buffeted and were moved to other locations outside the flow stream for these tests. The ground-plane microphones measured flyover noise data, simulating the case in which the aircraft flies directly over an observer on the ground. The flyover plane is shown in figure 9 as the plane AA'B'B. The angle $\theta_F$ is measured from the flight path AA' to the line $O_FP$, defined by the position of the flyover observer at point $O_F$ and the aircraft at point P. The QCSEE in-flight noise goals, however, are specified for a 152-m (500-ft) sideline flyby, as shown in figure 10. The sideline plane is the plane AA'C'C in figure 9. The angle $\theta_S$ is measured in the sideline plane from AA' to the line $O_SP$, defined by the sideline observer at $O_S$ and the aircraft at P. To obtain sideline

noise data, five microphones were hung from a cable suspended from two towers, all lying in a plane 90° to the engine axis at the nozzle exit as shown in figure 8(a). The microphones were spaced to provide proper angles relative to a ground observer at a 152-m (500-ft) sideline and an aircraft at altitudes of 0, 30.5, 61, 91.4, and 122 m (0, 100, 200, 300, and 400 ft, table IV). A sixth microphone was located to represent a sideline observer at 120° from the engine inlet with the aircraft at 61 m (200 ft), the estimated location of maximum sideline flyby noise.

Bruel and Kjaer 1.27-cm (0.5-in.) diameter condenser microphones equipped with windscreens were used. The ground-plane microphones were secured to 1.2- by 1.2-m (4- by 4-ft) hardboards, with microphones pointed nominally toward the noise source. The paved asphalt test area surface was painted white, except for the region within 15.2 m (50 ft) of the engine center, to minimize acoustic reflections due to temperature gradients near the asphalt surface.

## Experimental Methods

Aerodynamic and acoustic data were obtained over a range of corrected fan speeds from 81 to 95 percent of rated. The fan blade angle was varied from +5.2° to -7.6°, and the exhaust nozzle area was varied from 1.87 to 1.52 $m^2$ (2900 to 2350 $in^2$) in order to simulate both approach and takeoff power conditions as shown in the following table:

| Power condition | Corrected speed, percent of rated | Exhaust nozzle area | | Fan blade angle, deg |
|---|---|---|---|---|
| | | $m^2$ | $in^2$ | |
| Approach | 95 | 1.87 | 2900 | +5.2 |
| Takeoff | [a]95 | 1.52 | 2350 | -7.6 |

[a]Takeoff rated speed was limited by turbine inlet temperature.

The acoustic instrumentation and data recording system had a flat response over the frequency range of interest (25 to 16 000 Hz). Data signals were FM recorded from all channels simultaneously on magnetic tape. Each of the three samples for a given corrected fan speed was reduced separately by using a 1/3-octave-band analyzer and a 4-sec averaging time. The resulting sound pressure levels were arithmetically averaged and adjusted to standard-day atmospheric conditions (77° F, 70 percent relative humidity), and then sideline perceived noise levels were calculated by using the standardized procedures presented in reference 15.

The ground reflection characteristics of each of the overhead microphones were unique, and a spectral correction for each was empirically determined (refs. 3 and 7) and applied in cases where precise absolute values were desired or where comparisons between overhead microphones were to be made. This ground reflection correction is summarized in the next section.

## GROUND REFLECTION CORRECTION FOR THE QCSEE OVERHEAD MICROPHONE SYSTEM

The overhead microphone array (table V and fig. 8) is the key portion of the QCSEE acoustic measurement system since it provides the basic input for

the calculation of QCSEE in-flight sideline noise levels. This overhead array was also useful in determining the noise asymmetry of the complete engine-nozzle-wing system. The QCSEE engine noise spectra also included very significant low-frequency noise contributions from the combustor, jet, and jet flap, with jet-flap noise peaking well below 50 Hz. Thus spectral distortion due to ground reflections for very low frequencies could not be ignored.

Initially a computer program of the analytical model of reference 16 was employed to correct the overhead microphone data for a variety of source distributions. This model assumed a perfectly reflecting ground plane. These calculations indicated that the net effect of the reflected signal would be an increase of 1.9 dB for the entire spectrum. However, for detailed spectral comparisons made in reference 7, data were available from tests with the UTW engine alone so that an empirical correction could be made. This engine is axisymmetric, with the possible exception of the four-flap variable exhaust nozzle and an inlet slip-ring strut, neither of which should have more than a slight effect on symmetry about the engine axis of rotation. Corrections derived from these data include complicated effects that might be due to the engine itself, to the engine test stand structure, or to the presence and location of peripheral support equipment (fig. 8).

The pertinent acoustic measurements during the engine-wing tests were made at five overhead locations in a plane perpendicular to the engine axis at $90^{\circ}$ from the inlet ($\theta_S = 90^{\circ}$) and also at $90^{\circ}$ from the engine inlet in the ground-plane array ($\theta_F = 90^{\circ}$). In addition the $120^{\circ}$, 61-m (200-ft) overhead microphone and the $120^{\circ}$ ground microphone were important since the UTW engine was aft-noise dominated. A free-field spectrum was arrived at by subtracting 6 dB from the measured ground-plane SPL values over the entire spectrum. The spectral correction from the engine-alone data for each overhead ($\theta_S = 90^{\circ}$) microphone was then obtained by subtracting each 1/3-octave-band SPL value from the corresponding free-field value obtained from the $90^{\circ}$ ground-plane microphone or the $120^{\circ}$ ground-plane microphone in the case of the $120^{\circ}$, 61-m (200-ft) overhead microphone. Six representative test points were selected in which engine power settings varied from approach to takeoff conditions and for which postcalibration tests indicated high-quality data for the overhead system and for the $90^{\circ}$ and $120^{\circ}$ ground-plane microphones. Correction values for the six overhead microphones, which are given in table V, are the arithmetic means of the corrections from the six test runs. Also listed is the probable error of the mean values. The measured correction values above 1000 Hz for the 91.4- and 122-m (300- and 400-ft) altitude microphones are larger than the expected average correction of about -2 dB and may indicate the presence of additional reflection paths.

Tabulated corrections are given in table VI for PNL and OASPL for representative takeoff and approach power settings. As can be seen, the ground reflection corrections vary from -0.2 to -2.8 for OASPL and from -0.9 to -3.7 on a PNL basis. These corrections are not incorporated in the tables of data in this report.

## NEAR-FIELD EFFECTS ON TOWER MICROPHONES

Although it is desirable to measure far-field acoustic data at a distance of some 50 source diameters, it is not always possible. Interpretation of acoustic data obtained for widely distributed sources in a limited test area where this criterion cannot be met requires some caution. In the engine-alone

case the ground-plane microphones were some 45.7 m (150 ft), or 24 engine exhaust diameters, from the source. The overhead microphones at $90^{o}$ from the engine were typically some 25.3 m (83 ft), or about 13 diameters, away from the source, and the $120^{o}$, 61-m (200-ft) overhead microphone were about 17.7 m (58 ft), or only 9.3 diameters, away. However, in the powered-lift mode the high end of the trailing-edge flap was a principal noise source and was relatively close to the overhead microphones, with the $120^{o}$, 61-m (200-ft) microphone of the overhead system less than 12.8 m (42 ft) from the high end of the flap trailing edge. The edge was approximately 12.7 m (41.7 ft) from the engine inlet. Considering this inlet-to-flap-trailing-edge distance as the characteristic length of the powered-lift source, the overhead microphones were only 1 or 2 such lengths away.

Because of the questionable microphone and source geometry, anechoic chamber tests were conducted on a 1/17-scale model of the QCSEE UTW wing-flap configuration to determine corrections to the "far-field" noise associated with "close-in" measurement of jet-flap interaction noise. Data were obtained in the flyover plane at radiation angles $\theta_F$ of $90^{o}$ and $120^{o}$ from the engine inlet (fig. 9). In addition, similar tests were run at radiation angles $\theta_S$ of $90^{o}$ and $120^{o}$, simulating the 61-m (200-ft) altitude sideline condition with a simulated ground plane in position.

These tests indicated that very small corrections were required in the flyover-plane microphone data ($\varphi = 0^{o}$) at $\theta_F = 90^{o}$ either with the engine alone or with takeoff or approach flaps. Somewhat larger variations were measured for the sideline flyby microphone system. Small spectral corrections[1] were determined for the low-frequency jet-flap noise portion of the $90^{o}$, 61-m (200-ft) sideline ($\varphi = 68.2^{o}$) microphone. The near-field effect amounted to an increase of 0.5 dB for the approach flap and 0.3 dB for the takeoff flap configuration (within the normal accuracy (±1 dB) of the data). For the $120^{o}$, 61-m (200-ft) microphone ($\varphi = 68.2^{o}$) in the sideline plane, however, a very large increase of more than 7 PNdB was exhibited for the jet-flap noise with approach flaps and about 5 PNdB with takeoff flaps.

Since the measured spectrum at the $120^{o}$, 61-m (200-ft) ($\varphi = 68.2^{o}$) sideline microphone is a combination of spacially distributed, relatively close jet-flap noise and engine noise from a more distant source, the complexity of the problem precludes a simple corrective procedure. It was decided therefore to avoid use of the $120^{o}$, 61-m (200-ft) microphone data for the configurations that included the wing-flap because of the unacceptably large uncertainty of the data.

The corrections presented herein are based on the author's considered judgment derived from experience with the data analyses and the particular sound arena. It is recommended that the corrections be applied wherever detailed sound measurements are required.

## PRESENTATION OF DATA

The narrowband data plots and the 1/3-octave-band plots selected for presentation correspond to the parametric variables presented in table VII. All of the figures presented herein are for representative takeoff and

---

[1]The near-field effect tended to increase the noise measurement so that corrections should be subtracted from measured values to yield far-field noise.

approach engine power levels for the engine alone and for the respective power level to match each wing-flap configuration; that is, approach power for the approach wing-flap configuration and takeoff power for the two takeoff wing-flap configurations.

For the 30-Hz narrowband spectra, noise data from one sideline-plane microphone and one flyover-plane microphone for each configuration are presented in figure 11.

For the 1/3-octave-band spectra, 30.5-m (100-ft) radius lossless data from as many as four sideline-plane microphones and as many as five flyover-plane microphones (fig. 12) are presented. In the data tables (also 305-m (100-ft) radius lossless data) in this report, the data are as recorded except that the effect of absorption was removed for the conditions that prevailed at the test site and the data were adjusted to a standard radius of 30.5 m (100 ft). All of the data taken during the UTW program at Lewis are presented in table VIII, which is included on microfiche at the end of this report. Table III identifies configurations for each subset number in the tabulation.

## DISCUSSION

Although in a "data" report it is not customary to discuss in detail any results, some of the data presented are unusual in their behavior and invite some general comments.

The narrowband data presented in figure 11 are somewhat unusual. The engine-alone, approach-power noise data for the three microphones (figs. 11(d), (e), and (f)) all exhibit extra modulated tones that appear at frequencies approximately 200 Hz greater than the blade passing frequency (BPF) harmonics. A one-per-revolution output by the core compressor (12 153 rpm) could explain this behavior.

The narrowband data for takeoff power and for the wing and both takeoff flap configurations also show somewhat unusual SPL minima and maxima (ignoring the BPF and harmonic spikes) that are apparent for the flyover-plane (ground-plane microphone) results (figs. 11(h), (i), (k), and (l)) but not for the sideline-plane (overhead microphone results) (figs. 11(g) and (j)). These minima and maxima occur in a regular progression and are probably due to sound wave cancellation and reinforcement phenomena that occur when sound originates from more than one source and is reflected from more than one surface. In this case fan, core, and jet-flap noise are reflected by the wing-flap system and other surfaces such as the thrust stand and instrumentation boxes (fig. 8). This provides several sound paths to the ground-plane microphones but not to the tower microphones, which are not in the direct reflection zone.

The same type of reflection phenomena are shown in the 1/3-octave-band plots of figure 12. Since these data are corrected to the same 30.5-m (100-ft) radius, direct comparisons can be made between levels of flyover-plane and sideline-plane noise data. In this series of plots, figure 12(e) can be compared with 12(f) ($20^{\circ}$ flap), figure 12(g) with 12(h) ($30^{\circ}$ flap), and figure 12(i) with 12(j) ($60^{\circ}$ approach flap). Note the regular behavior of the SPL data for the four sideline-plane microphones (fig. 12(i)) at frequencies above 1000 Hz (BPF). Contrast that with the flyover-plane SPL data above the same frequency for the three microphones at $\theta_F$ of $30^{\circ}$, $60^{\circ}$, and $90^{\circ}$ (fig. 12(j)). The $150^{\circ}$ data are smooth, but this microphone location was beyond the wake of the engine-wing-flap system and therefore beyond most of the reflection zone. Referring to the sketch of figure 8 also helps to show that the $150^{\circ}$ ground-plane microphone is out of the reflection zone of the wing-flap system.

## APPENDIX - SYMBOLS

| | |
|---|---|
| $A_{18}$ | exhaust nozzle area, ($in^2$) |
| D | engine fan exhaust nozzle diameter (1.9 m) |
| DISTANCE | distance in feet measured from engine axis directly to microphone (fig. 8) |
| FGK | gross thrust measurement corrected for ambient wind velocity and direction, lb |
| FREQ. | frequency for 1/3-octave band, Hz |
| F.S. | fully suppressed engine |
| MIC# | microphone number |
| OASPL | overall sound pressure level |
| PHI | angle from vertical flyover plane to sideline (fig. 9) |
| R | radius measured from directly over engine to the tower microphone (fig. 8), ft |
| SDOF | single degree of freedom |
| SPL | sound pressure level, dB |
| THETA ($\theta_F$) | angle from flight path or engine centerline to observer in flyover plane (fig. 9), deg. |
| THETA ($\theta_S$) | angle from flight path or engine centerline to observer in sideline plane (fig. 9), deg. |
| X | nozzle-to-flap distance measured along engine centerline |
| X/D | nozzle-to-flap separation distance ratio |
| XM11 | average inlet throat Mach number |
| Z | vertical distance measured from ground to tower microphones (fig. 8), ft |
| $\beta_F$ | fan blade angle measured from reference design angle, deg |

## REFERENCES


1. Ciepluch, C.C.: A Review of the QCSEE Program. NASA TM X-71818, 1975.

2. Ciepluch, C.C.: Overview of the QCSEE Program. Powered-Lift Aerodynamics and Acoustics. NASA SP-406, 1976, pp. 325-333.

3. Loeffler, I.J.; Samanich, N.E.; and Bloomer, H.E.: QCSEE UTW Engine Powered-Lift Acoustic Performance. AIAA Paper 80-1065, June 1980.

4. Quiet, Clean, Short-Haul Experimental Engine (QCSEE) Under the Wing (UTW) Design Report. (General Electric Co.; NASA Contract NAS3-18021.) NASA CR-134847, 1977.

5. Stimpert, D.L.: Quiet, Clean, Short-Haul Experimental Engine (QCSEE) Under-the-Wing (UTW) Composite Nacelle Test Report. Vol. 2: Acoustic Performance. (R78AEG574-Vol-2, General Electric Co., NASA Contract NAS3-18021.) NASA CR-159472, 1979.

6. Bloomer, H.E.; and Samanich, N.E.: QCSEE Fan Exhaust Bulk Absorber Treatment Evaluation. AIAA Paper 80-0987, June 1980. Also NASA TM-81498.

7. Bloomer, H.E.; et al.: Comparison of NASA and Contractor Results from Aeroacoustic Tests of QCSEE OTW Engine. NASA TM-81761, 1981.

8. Clemons, A.: Quiet, Clean, Short-Haul Experimental Engine (QCSEE): Acoustic Treatment Development and Design. (R76AEG379-1, General Electric Co.; NASA Contract NAS3-18021.) NASA CR-135266, 1979.

9. Loeffler, I.J.; Smith, E.B.; and Sowers, H.D.: Acoustic Design of the QCSEE Propulsion Systems. Powered-Lift Aerodynamics and Acoustics, NASA SP-406, 1976, pp. 335-356.

10. "Quiet Clean Short-Haul Experimental Engine (QCSEE) Under-the-Wing Engine Digital Control System Design Report. (R75AEG483, General Electric Co.; NASA Contract NAS3-18021.) NASA CR-134920, 1978.

11. McKinzie, Daniel J., Jr.: Measured and Predicted Impingement Noise for a Model-Scale Under-the-Wing Externally Blown Flap Configuration with a QCSEE-Type Nozzle. NASA TM-81494, 1980.

12. Whitcomb, R.T.: Review of NASA Supercritical Airfoils. ICAS Paper 74-10, Aug. 1974.

13. McKinzie, Daniel J., Jr.; and Burns, Robert J.: Analysis of Noise Produced by Jet Impingement Near the Trailing Edge of a Flat and a Curved Plate. NASA TM X-3171, 1975.

14. McKinzie, Daniel J., Jr.; Burns, Robert J.; and Wagner, Jack M.: Noise Reduction Tests of Large-Scale-Model Externally Blown Flap Using Trailing-Edge Blowing and Partial Flap Slot Covering. NASA TM X-3379, 1976.

15. Montegani, F.J.: Some Propulsion System Noise Data Handling Conventions and Computer Programs Used at the Lewis Research Center. NASA TM X-3013, 1974.

16. Putnam, T.W.: Review of Aircraft Noise Propagation. NASA TM X-56033, 1975.

TABLE I. - ACOUSTIC DESIGN PARAMETERS FOR UTW ENGINE

(91.4-m/sec (80-knot) aircraft speed; 61-m (200-ft) altitude, takeoff conditions.)

| | |
|---|---|
| Number of fan blades | 18 |
| Fan diameter, $D_f$, cm (in.) | 180.4 (71) |
| Fan pressure ratio | 1.27 |
| Fan speed, rpm | 9089 (3744 at 100%) |
| Fan tip speed, m/sec (ft/sec) | 289.6 (950) |
| Number of outlet guide vanes | 33 (32 + pylon) |
| Fan weight flow (corrected), kg/sec (lbm/sec) | 405.5 (894) |
| Inlet Mach number (throat) | 0.75 |
| Rotor OGV spacing, rotor tip aerodynamic chords | 1.5 |
| Fan exhaust area, $m^2$ ($in^2$) | 1.615 (2504) |
| Core exhaust area, $m^2$ ($in^2$) | 0.348 (540) |
| Gross thrust (sea-level static uninstalled), kN (lb) | 81.39 (18 300) |
| Blade passing frequency, Hz | 927 |
| Core exhaust flow, kg/sec (lbm/sec) | 31.3 (69.1) |
| Fan exhaust velocity, m/sec (ft/sec) | 197.8 (649) |
| Core exhaust velocity, m/sec (ft/sec) | 238.9 (784) |
| Bypass ratio | 12.1 |
| Ratio of inlet treatment length to fan diameter, $L_T/D_f$ | 0.74 |
| Vane-blade ratio | 1.83 |

TABLE II. - NOMINAL CONDITIONS (AS TESTED)

| Condition | Takeoff | Approach |
|---|---|---|
| Corrected fan speed, percent | 95 | 95 |
| Fan exhaust area, $m^2$ ($in^2$) | 1.516 (2350) | 1.670 (2900) |
| Core exhaust area, $m^2$ ($in^2$) | 0.348 (540) | 0.348 (540) |
| Fan blade angle (panel + 28°), deg | -7.6 | -5.2 |
| Corrected gross thrust (installed), kN (lbf) | 77.39 (17 400) | 55.42 (12 460) |
| Inlet throat Mach number (one dimensional) | 0.75 | 0.63 |
| Fan pressure ratio | 1.25 | 1.14 |
| Bypass ratio | 11.7 | 12.6 |
| Fan exhaust velocity, m/sec (ft/sec) | 195 (640) | 151 (495) |
| Core exhaust velocity, m/sec (ft/sec) | 253 (830) | 177 (580) |
| Mass average velocity, m/sec (ft/sec) | 200 (655) | 152 (500) |

TABLE III. - CONFIGURATIONS AND DATA TABULATION IDENTIFICATION FOR QCSEE UTW ACOUSTIC TEST CONFIGURATIONS

| Engine wing-flap configuration | Data tabulation | | Inlet type | Inlet treatment type | Frame treatment ? | Fan duct treatment type | Acoustic splitter ? | Core treatment | Wing-flap configuration (fig. 7) | Slip-ring strut installed ? |
|---|---|---|---|---|---|---|---|---|---|---|
| | Configuration | Subsets | | | | | | | | |
| 1 | 010 | 164-173 | Hybrid | SDOF[a] | Yes | Phased SDOF | Yes | Yes | None | Yes |
| [b]1 | 010 | 174-183 | | | | | | | None | No |
| 1A | 011 | 135-139 | | | | | | | Cruise | Yes |
| 1B | 012 | 140-147 | | | | | | | 20° takeoff flap | |
| 1C | 013 | 148-153 | | | | | | | 30° takeoff flap | |
| 1D | 014 | 154-161 | | | | | | | 60° Approach flap | |
| [b]1D | 014 | 162-163 | | | | | | | 60° Approach flap | No |
| 2B | 022 | 193-197 | | | | | No | No | 20° takeoff flap | Yes |
| 2D | 024 | 184-189 | | | | | | | 60° Approach flap | |
| [c]2D | 024 | 190-192 | | | | | | | 60° Approach flap | |
| 6 | 040 | 209-214 | Bellmouth | Hard | | Hard | | | None | |
| 6C | 043 | 198-203 | Bellmouth | Hard | | Hard | | | 30° takeoff flap | |
| 6D | 044 | 204-208 | Bellmouth | Hard | | Hard | | | 60° takeoff flap | |
| 3 | 050 | 215-219 | Hybrid | SDOF | | Bulk absorber | Yes | | None | |
| 2 | 070 | 121-134 | | | | Phased SDOF | | | | |
| 4 | 080 | 220-223 | | | | Bulk absorber taper | | | | |
| 5 | 090 | 224-228 | | | | Bulk absorber front half taped | | | | |

[a] Single degree of freedom.
[b] Special tests run without slip-ring strut in inlet to check effect on forward-quadrant microphones.
[c] Special test run without crossbeam support from wing to flap to check effect on tower microphones.

TABLE IV. - OVERHEAD (SIDELINE PLANE) MICROPHONE PLACEMENT

| Sideline angle[a], $\theta_S$, deg | Altitude | | Distance[a] | | Ground plane radius[a], R | | Height above ground plane, z | | Angle from vertical flyover plane to microphone[a], $\phi$, deg |
|---|---|---|---|---|---|---|---|---|---|
| | m | ft | m | ft | m | ft | m | ft | |
| 90 | 0 | 0 | 27.6 | 90.6 | 0 | 0 | 32.3 | 106 | 0 |
| 90 | 30.5 | 100 | 25.8 | 84.6 | 5.2 | 17 | 29.9 | 98 | 11 |
| 90 | 61 | 200 | 24.9 | 81.8 | 9.4 | 31 | 27.7 | 91 | 22 |
| 90 | 91.4 | 300 | 25.2 | 82.6 | 13.1 | 43 | 26.2 | 86 | 31 |
| 90 | 122 | 400 | 26.1 | 85.6 | 16.5 | 54 | 24.7 | 81 | 39 |
| 120 | 61 | 200 | 17.7 | 58.1 | 10.4 | 34 | 19.2 | 63 | 35 |

[a]See fig. 8.

TABLE V. - MEASURED TEST AREA REFLECTIVITY CORRECTIONS FOR OCSEE OVERHEAD MICROPHONE SYSTEM

| Frequency, Hz | Sideline angle, $\theta_S$, deg | | | | | | | | | | | |
|---|---|---|---|---|---|---|---|---|---|---|---|---|
| | 90 | | | | | | | | | | 120 | |
| | Altitude, m (ft) | | | | | | | | | | | |
| | 0 | | 30.5 (100) | | 61.0 (200) | | 91.4 (300) | | 121.9 (400) | | 61.0 (200) | |
| | Corrections to be added to measured values (table VIII) | | | | | | | | | | | |
| | ΔdB | PE[a] | ΔdB | PE | ΔdB | PE | ΔdB | PE | ΔdB | PE | ΔdB | PE |
| 75 | -2.1 | 0.7 | -0.9 | 0.6 | 1.3 | 0.3 | -0.7 | 0.3 | -1.2 | 0.4 | 0.3 | 1.7 |
| 31.5 | -2.1 | .2 | -1.2 | .4 | .5 | .2 | -1.5 | .2 | -1.9 | .6 | -.3 | 1.1 |
| 40 | -1.3 | .3 | -.6 | .5 | .7 | .5 | -.3 | .4 | -.8 | .4 | -.2 | 1.3 |
| 50 | -1.2 | .4 | -1.3 | .5 | .6 | .4 | .3 | .4 | -.9 | .3 | -.3 | .9 |
| 63 | -.9 | .2 | -1.1 | .4 | -.2 | .5 | -.7 | .4 | -3.0 | .4 | -1.4 | .8 |
| 80 | -.9 | .3 | -.9 | .5 | -.5 | .4 | -.6 | .2 | -1.8 | .3 | -.5 | .6 |
| 100 | .5 | .4 | -.1 | .4 | -.0 | .4 | -.6 | .3 | -1.0 | .2 | -1.2 | .8 |
| 125 | -.4 | .2 | -1.0 | ↓ | -.6 | .3 | -1.3 | .3 | -1.5 | .2 | -.2 | .7 |
| 160 | .5 | .4 | -.4 | ↓ | -.6 | .3 | -1.0 | .4 | -2.2 | .3 | -1.0 | .6 |
| 200 | 1.7 | .4 | 1.0 | ↓ | .9 | .4 | .3 | .5 | .0 | .4 | -1.7 | .9 |
| 250 | -.5 | .2 | -.5 | .3 | -1.5 | .4 | -1.6 | .3 | -2.2 | ↓ | -.3 | .3 |
| 315 | -.4 | .2 | -.5 | .1 | -1.7 | .3 | -1.8 | .3 | -2.6 | ↓ | .0 | 1.1 |
| 400 | .6 | .1 | -.1 | .1 | -2.0 | .2 | -1.8 | .2 | -2.4 | ↓ | .5 | .6 |
| 500 | -1.7 | .2 | -1.5 | .2 | -2.7 | .1 | -3.3 | .3 | -3.9 | ↓ | 1.1 | 1.1 |
| 630 | -.9 | .1 | .2 | .2 | -1.2 | .1 | -2.0 | .2 | -2.4 | .1 | .4 | .8 |
| 800 | .9 | .2 | .1 | .2 | -1.0 | .2 | -1.1 | .2 | -2.3 | .3 | -.6 | 1.3 |
| 1 000 | -.7 | .4 | -.7 | .5 | -2.4 | .4 | -3.2 | .4 | -3.3 | .5 | -.4 | 1.1 |
| 1 250 | .6 | .2 | -.1 | .1 | -1.5 | .2 | -2.3 | .1 | -3.1 | .2 | -.1 | .6 |
| 1 600 | -1.4 | .3 | -2.0 | .2 | -2.9 | .2 | -3.5 | .2 | -4.0 | .2 | -1.0 | .7 |
| 2 000 | -1.8 | .2 | -2.7 | ↓ | -3.9 | .3 | -4.4 | .3 | -4.9 | .4 | -.3 | .9 |
| 2 500 | -2.2 | ↓ | -2.8 | ↓ | -3.3 | .3 | -4.6 | .4 | -4.8 | .3 | -.6 | 1.1 |
| 3 150 | -1.3 | ↓ | -2.6 | ↓ | -2.7 | .2 | -4.0 | .3 | -4.6 | .3 | .1 | .5 |
| 4 000 | -.8 | ↓ | -1.9 | .3 | -1.8 | .2 | -3.8 | .3 | -4.3 | .4 | .6 | .2 |
| 5 000 | -1.3 | ↓ | -3.0 | .1 | -1.9 | .1 | -4.2 | .2 | -4.6 | .1 | .6 | .9 |
| 6 300 | -1.2 | ↓ | -3.4 | .2 | -1.6 | .2 | -4.9 | .2 | -4.6 | .2 | 1.4 | .5 |
| 8 000 | -.8 | ↓ | -3.8 | .2 | -1.3 | .2 | -5.5 | .1 | -4.9 | .2 | 1.1 | .5 |
| 10 000 | -.4 | .1 | -4.3 | .1 | -.3 | .2 | -5.7 | .1 | -5.5 | .1 | .4 | .4 |

[a]Probable error.

TABLE VI. - EFFECT OF GROUND REFLECTION CORRECTION ON MEASURED OASPL AND PNL OVER A RANGE OF POWERS FROM APPROACH TO TAKEOFF POWER

[Corrections are to be added to measured values (table VIII).]

| Sideline angle, $\phi_S$, deg | Simulated altitude of overhead microphone system | | Correction in OASPL, adB | Correction in PNL, adb |
|---|---|---|---|---|
| | m | ft | | |
| 90 | 0 | 0 | -0.. | -0.9 |
| | 30.0 | 100 | -1.1 | 1.8 |
| | 61.0 | 200 | -1.3 | -2.0 |
| | 91.4 | 300 | -2.2 | -3.3 |
| | 121.9 | 400 | -2.8 | -3.7 |
| 120 | 61.0 | 200 | *.2 | 0 |

TABLE VII. - CONDITIONS FOR NARROWBAND AND 1/3-OCTAVE-BAND PLOTS

[Rated fan speed for all points on table, 95 percent of design.]

| Data subset | Engine wing-flap configuration | Engine power setting | Fan blade angle, deg | Narrowband plots | | 1/3-Octave band plots | |
|---|---|---|---|---|---|---|---|
| | | | | Figure | Microphone location (refer to fig. 8) | Figure | Microphone location |
| 168 | 1 | Takeoff | -7.1 | 11(a) | $\phi_S$ = 90°, 91.4-m (300-ft) tower | 12(a) | Tower |
| | | | | 11(b) | $\phi_F$ = 120°, GP[a] | 12(b) | GP |
| | | | | 11(c) | $\phi_F$ = 90°, GP | | |
| 173 | 1 | Approach | +1.1 | 11(d) | $\phi_S$ = 90°, 91.4-m (300-ft) tower | 12(c) | Tower |
| | | | | 11(e) | $\phi_F$ = 120°, GP | 12(d) | GP |
| | | | | 11(f) | $\phi_F$ = 100°, GP | | |
| 144 | 18 | Takeoff | -7.5 | 11(g) | $\phi_S$ = 90°, 91.4-m (300-ft) tower | 12(e) | Tower |
| | | | | 11(h) | $\phi_F$ = 120°, GP | 12(f) | GP |
| | | | | 11(i) | $\phi_F$ = 90°, GP | | |
| 148 | 10 | Takeoff | -7.6 | 11(j) | $\phi_S$ = 90°, 91.4-m (300-ft) tower | 12(g) | Tower |
| | | | | 11(k) | $\phi_F$ = 120°, GP | 12(h) | GP |
| | | | | 11(l) | $\phi_F$ = 90°, GP | | |
| 155 | 10 | Approach | +0.6 | 11(m) | $\phi_S$ = 90°, 91.4-m (300-ft) tower | 12(i) | Tower |
| | | | | 11(n) | $\phi_F$ = 140°, GP | 12(j) | GP |

[a]Ground microphones, flyover plane.

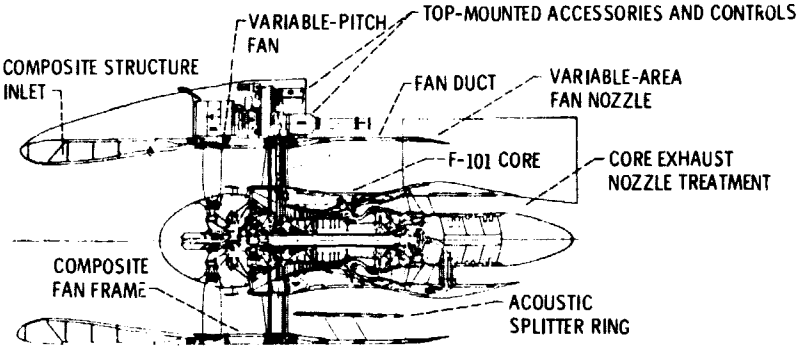


Figure 1. - UTW experimental propulsion system.

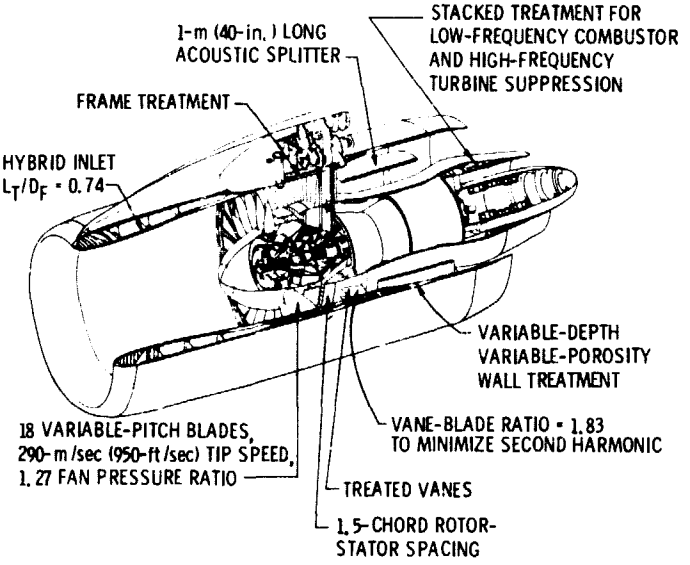


Figure 2. - Acoustic design features of QCSEE UTW engine.

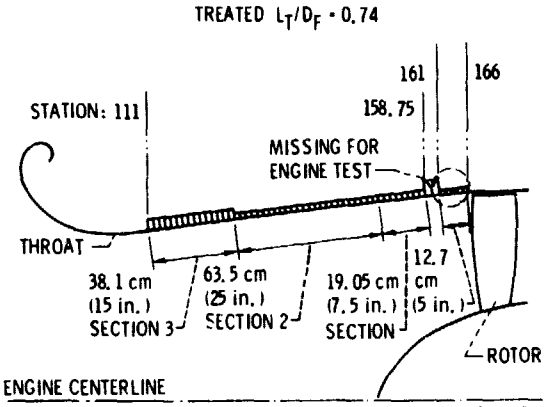


| SECTION | HOLE SIZE, cm (in.) | POROSITY, percent | CAVITY DEPTH, cm (in.) | FACEPLATE THICKNESS, cm (in.) |
|---|---|---|---|---|
| 1 | 0.1589 (0.0625) | 9.89 | 1.27 (0.50) | 0.0813 (0.032) |
| 2 | 0.1589 (0.0625) | 9.89 | 1.91 (0.75) | 0.0813 (0.032) |
| 3 | 0.1589 (0.0625) | 9.89 | 3.82 (1.50) | 0.0813 (0.032) |

| SECTION | DESIGN FREQUENCIES | |
|---|---|---|
| | REVERSE THRUST, Hz | FORWARD THRUST, Hz |
| 1 | 3150 | 2000 |
| 2 | 2500 | 1600 |
| 3 | 1600 | 1000 |

(a) Inlet treatment.

Figure 3. - Acoustic design details.

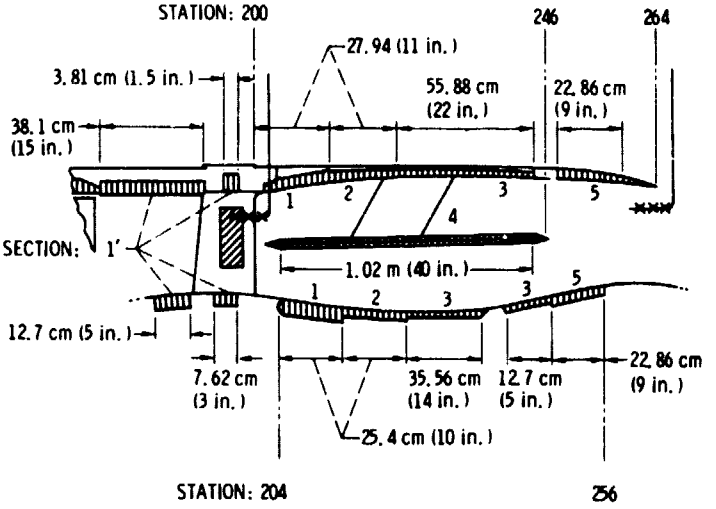


| | DEPTH, cm (in.) | POROSITY, % | HOLE SIZE, cm (in.) | FACEPLATE THICKNESS, cm (in.) | FREQUENCY, Hz |
|---|---|---|---|---|---|
| FAN FRAME TREATMENT | | | | | |
| SECTION 1' | 5.08 (2.0) | 10 | 0.1589 (0.0625) | 0.0869 (0.035) | 1000 |
| TREATED VANES | 0.76 (0.3) | 10 | 0.1589 (0.0625) | 0.127 (0.05) | 4000 |
| FAN EXHAUST TREATMENT | | | | | |
| SECTION 1 | 5.08 (2) | 22 | 0.1589 (0.0625) | 0.1016 (0.040) | 1250 |
| SECTION 2 | 2.54 (1) | 15.5 | 0.1589 (0.0625) | 0.1016 (0.040) | 2000 |
| SECTION 3 | 1.90 (0.75) | 15.5 | 0.1589 (0.0625) | 0.1016 (0.040) | 2500 |
| SECTION 4 | 1.27 (0.5) | 11.5 | 0.198 (0.078) | 0.2032 (0.080) | 2500 |
| SECTION 5 | 2.54 (1) | 15.5 | 0.1589 (0.0625) | 0.1016 (0.040) | 1600 |

(b) Composite nacelle fan exhaust duct treatment.

Figure 3. - Continued.

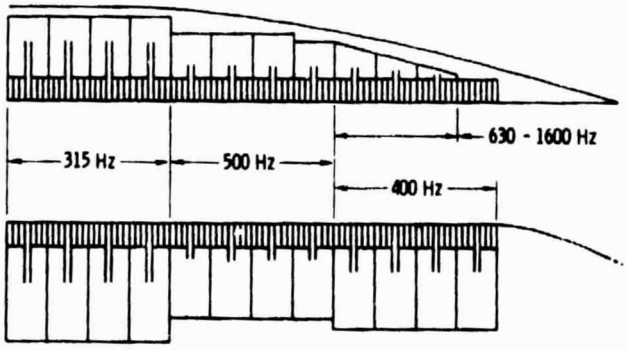


| | COMBUSTOR | | | | | | TURBINE, |
|---|---|---|---|---|---|---|---|
| | INNER WALL | | | OUTER WALL | | | BOTH WALLS |
| TUNING FREQUENCY, Hz | 315 | 400 | 500 | 315 | 500 | 630 - 1600 | 3150 |
| NECK LENGTH (FACEPLATE THICKNESS), cm (in.) | 6.99 (2.75) | 5.72 (2.25) | 4.45 (1.75) | 6.99 (2.75) | 4.45 (1.75) | 3.56 - 2.54 (1.4 - 1.0) | 0.08128 (0.032) |
| CAVITY DEPTH, cm (in.) | 10.2 (4.0) | 8.89 (3.5) | 7.62 (3.0) | 7.62 (3.0) | 4.32 & 5.08 (1.7 & 2) | 4.06 - 0.51 (1.6 - 0.2) | 1.905 (0.75) |
| POROSITY, % | 10 | 10 | 10 | 7 | 7 | 7 | 10 |
| TREATMENT LENGTH, cm (in.) | 20.32 (8.0) | 20.32 (8.0) | 20.32 (8.0) | 20.32 (8.0) | 15.24 & 5.08 (6.0 & 2.0) | 20.32 (8.0) | 60.96 (24.0) |
| HOLE DIAM., cm (in.) | 1.52 (0.6) | 1.52 (0.6) | 1.52 (0.6) | 1.52 (0.6) | 1.52 (0.6) | 1.52 (0.6) | 0.1575 (0.062) |

(c) Core exhaust treatment.

Figure 3. - Concluded

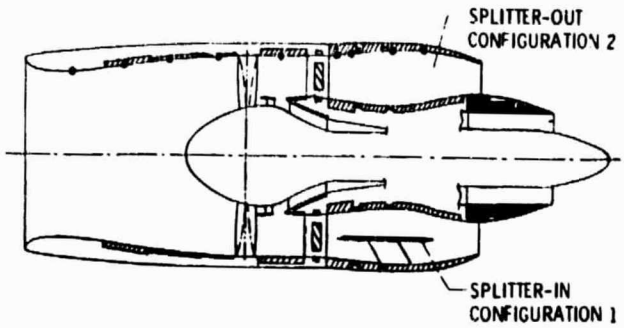


Figure 4. - Fully suppressed configuration, configuration 1. Without fan duct splitter, configuration 2.

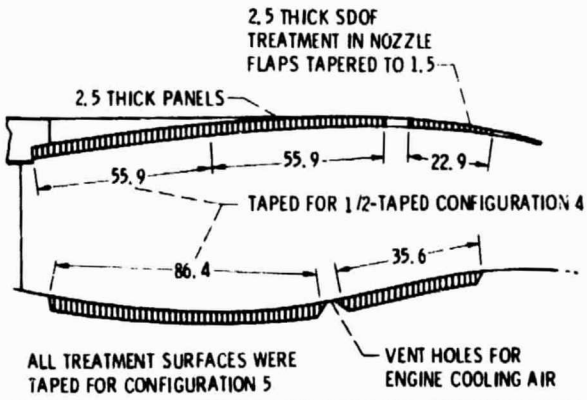


Figure 5. - Bulk absorber configuration 3 for UTW fan duct. Kevlar design density, 56 kg/m$^3$ (3.5 lb/ft$^3$); facing sheet porosity, 30 percent open; design tuning frequency, 1600 Hz. (All dimensions are in cm.)

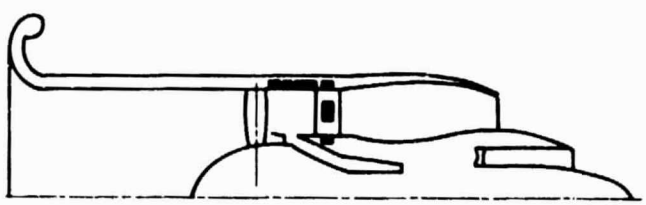

Figure 6. - Baseline engine configuration 6 with bellmouth inlet. (Untreated except for treated frame and vanes.)

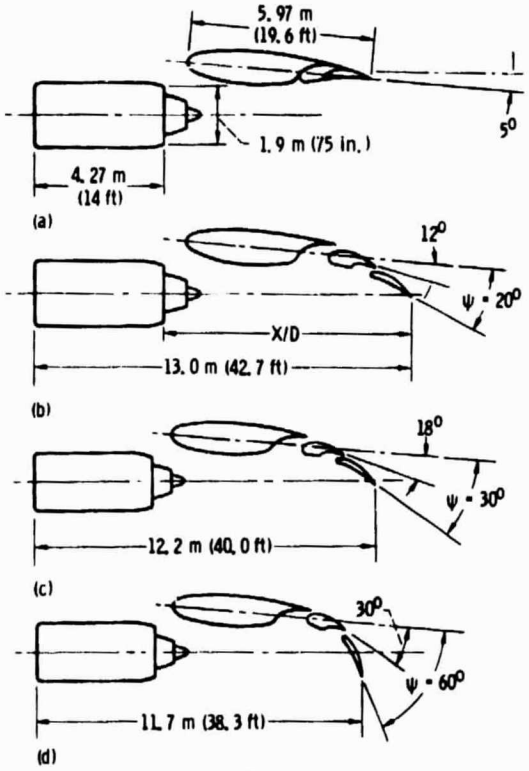


(a) Cruise.
(b) Takeoff, $\psi = 20^0$.
(c) Takeoff, $\psi = 30^0$.
(d) Approach, $\psi = 60^0$.

Figure 7. - UTW wing-flap configurations.

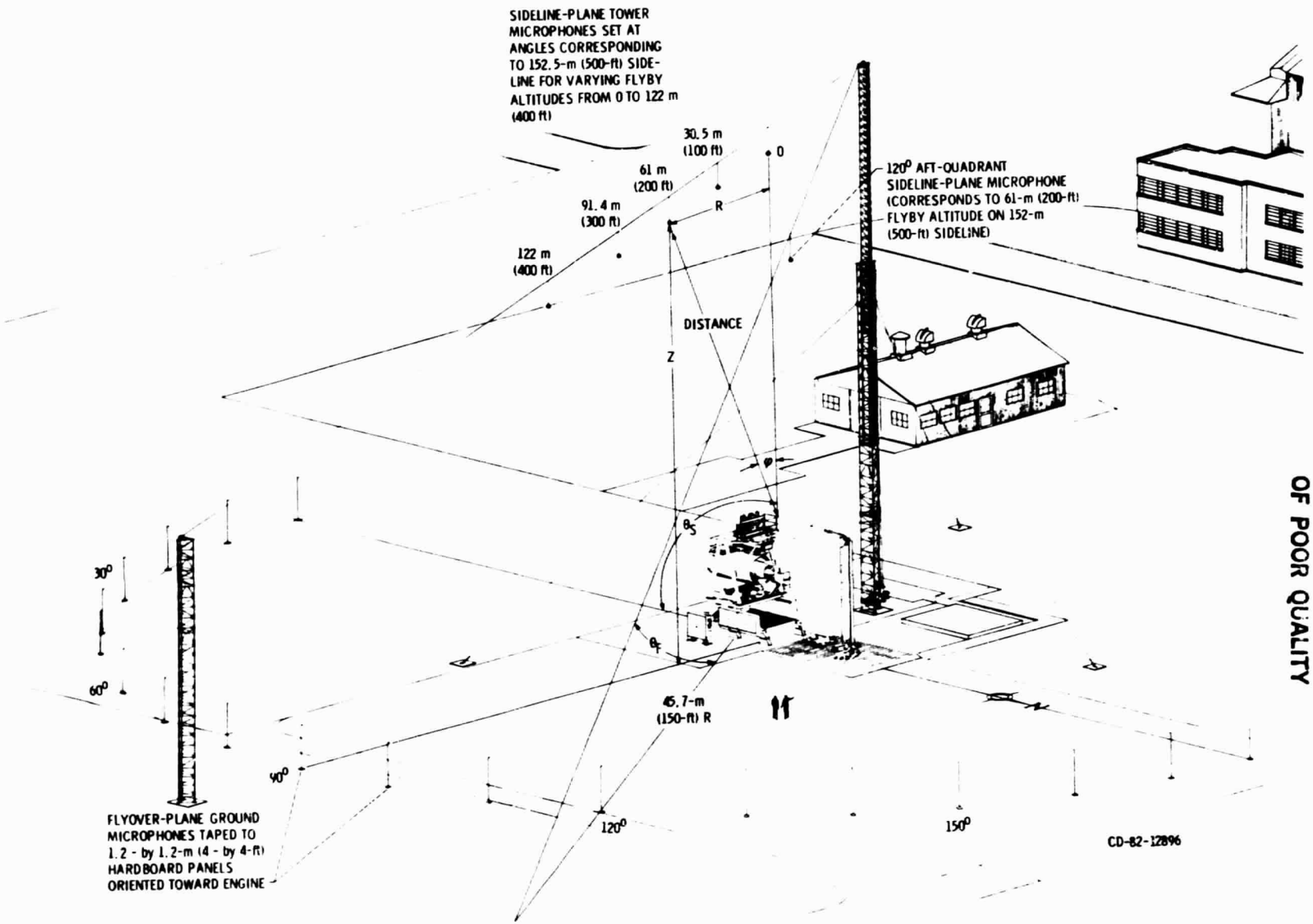


(a) Sketch showing microphone locations and main microphone tower extended.

Figure 8. - Engine noise test facility.

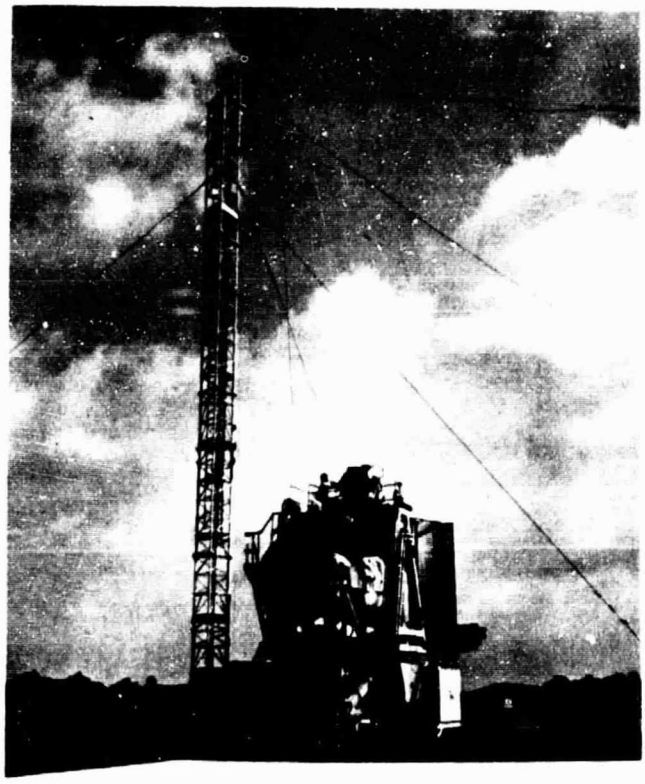

(b) Photograph showing engine stand and microphone tower in retracted position.

Figure 8. - Concluded.

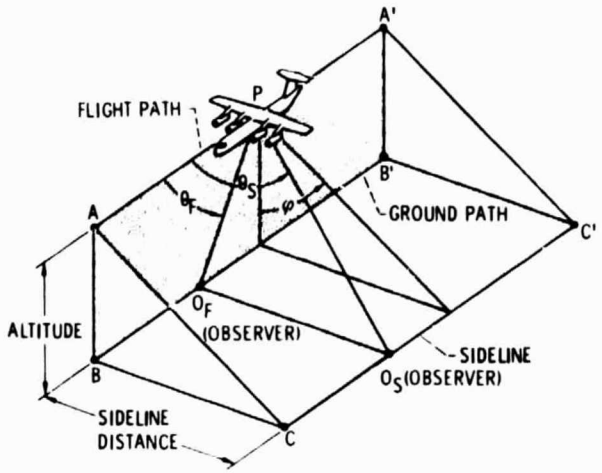


Figure 9. - Flyover and sideline flyby geometry.

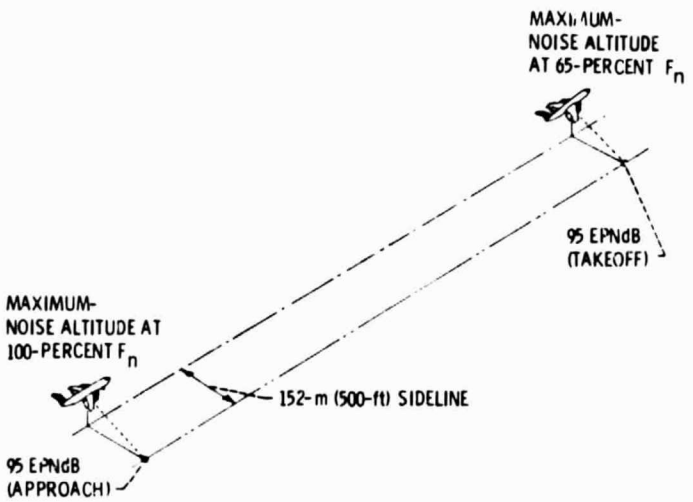


Figure 10. - QCSEE in-flight noise goals. Number of engines, 4; installed thrust, $F_n$, 400 kN (90 000 lb); runway length, 610 m (2000 ft).

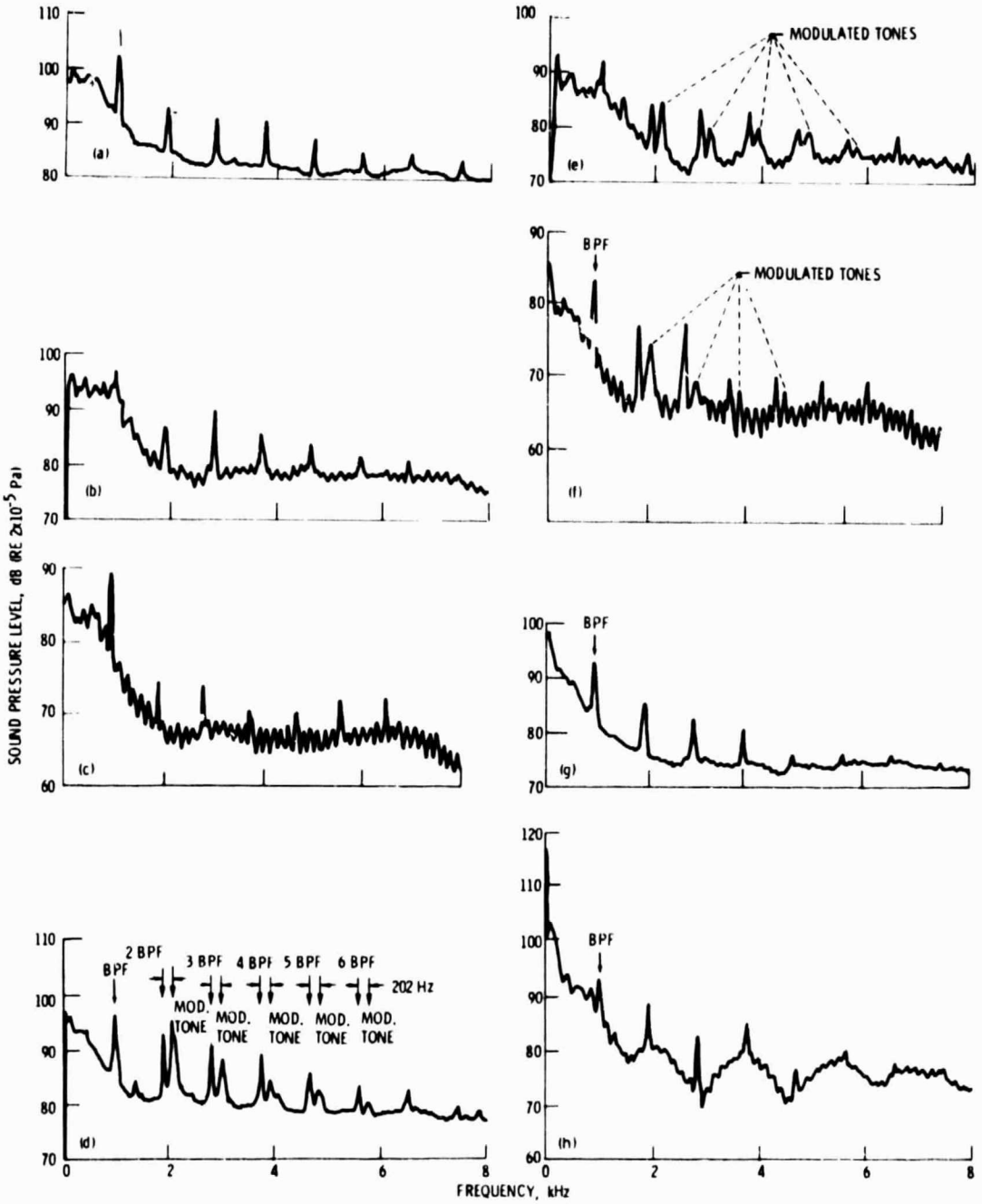


(a) Engine alone; takeoff power; 91.4-m (300-ft) altitude, sideline-plane microphone ($\theta = 90^{0}$ and $\phi = 31^{0}$).

(b) Engine alone; takeoff power; $120^{0}$ flyover-plane microphone.

(c) Engine alone; takeoff power; $90^{0}$ flyover plane microphone.

(d) Engine alone; approach power; 91.4-m (300-ft) altitude, sideline-plane microphone ($\theta = 90^{0}$ and $\phi = 31^{0}$).

(e) Engine alone; approach power; $120^{0}$ flyover-plane microphone.

(f) Engine alone; approach power; $100^{0}$ flyover-plane microphone.

(g) Engine with wing and $20^{0}$ takeoff flap; takeoff power; 91.4-m (300-ft) altitude, sideline-plane microphone.

(h) Engine with wing and $20^{0}$ takeoff flap; takeoff power; $120^{0}$ flyover-plane microphone.

Figure 11. - Narrowband spectra; filter bandwidth, 30 Hz.

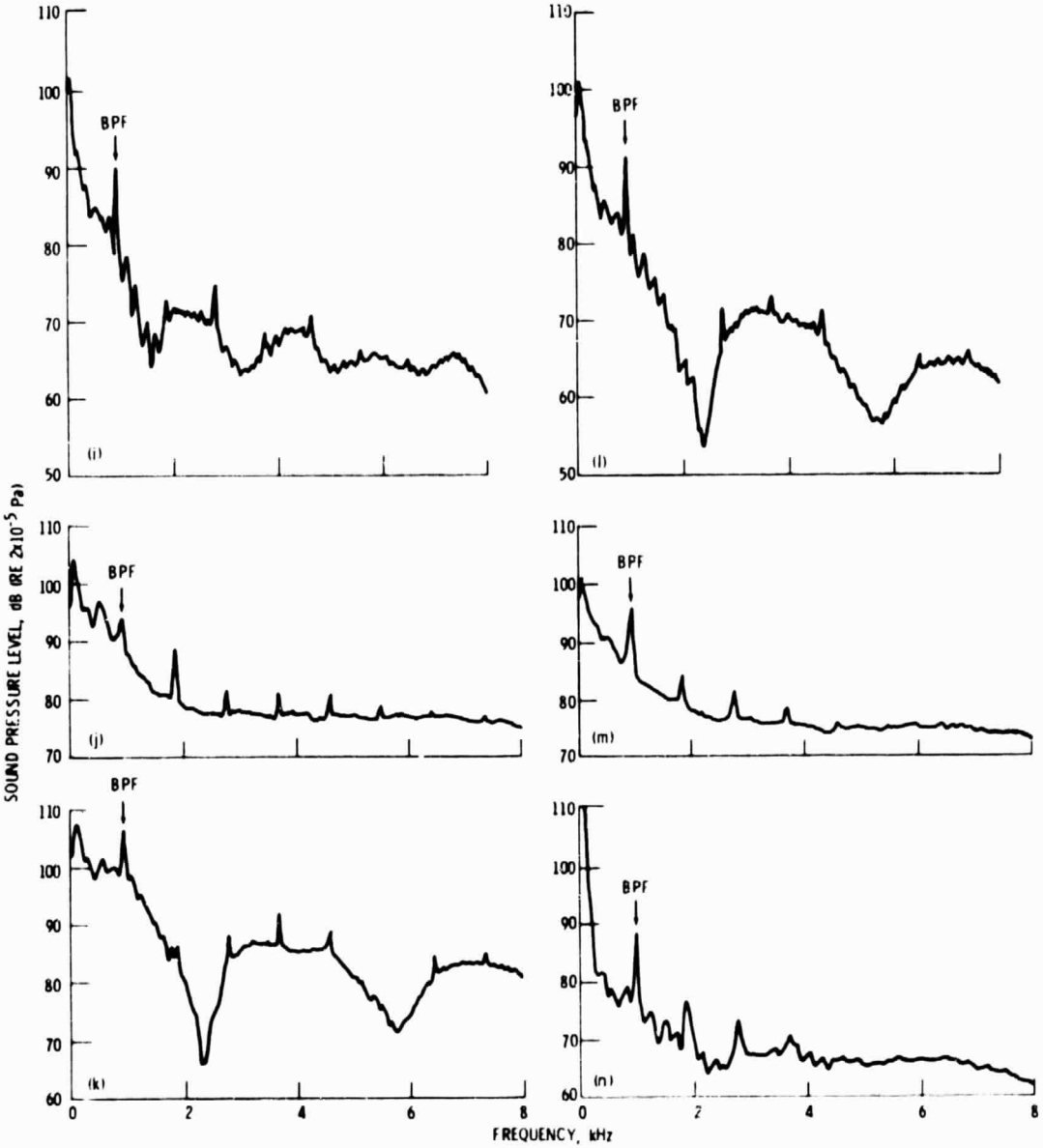


(i) Engine with wing and 20° takeoff flap; takeoff power; 90° flyover-plane microphone.

(j) Engine with wing and 30° takeoff flap; takeoff power; 91.4-m (300-ft) altitude, sideline-plane microphone ($\theta$ = 90° and $\phi$ = 31°).

(k) Engine with wing and 30° takeoff flap; takeoff power; 120° flyover-plane microphone.

(l) Engine with wing and 30° takeoff flap; takeoff power; 90° flyover-plane microphone.

(m) Engine with wing and 60° approach flap; approach power; 91.4-m (300-ft) altitude, sideline-plane microphone ($\theta$ = 90° and $\phi$ = 31°).

(n) Engine with wing and 60° approach flap; approach power; 140° flyover-plane microphone.

Figure 11. - Concluded.

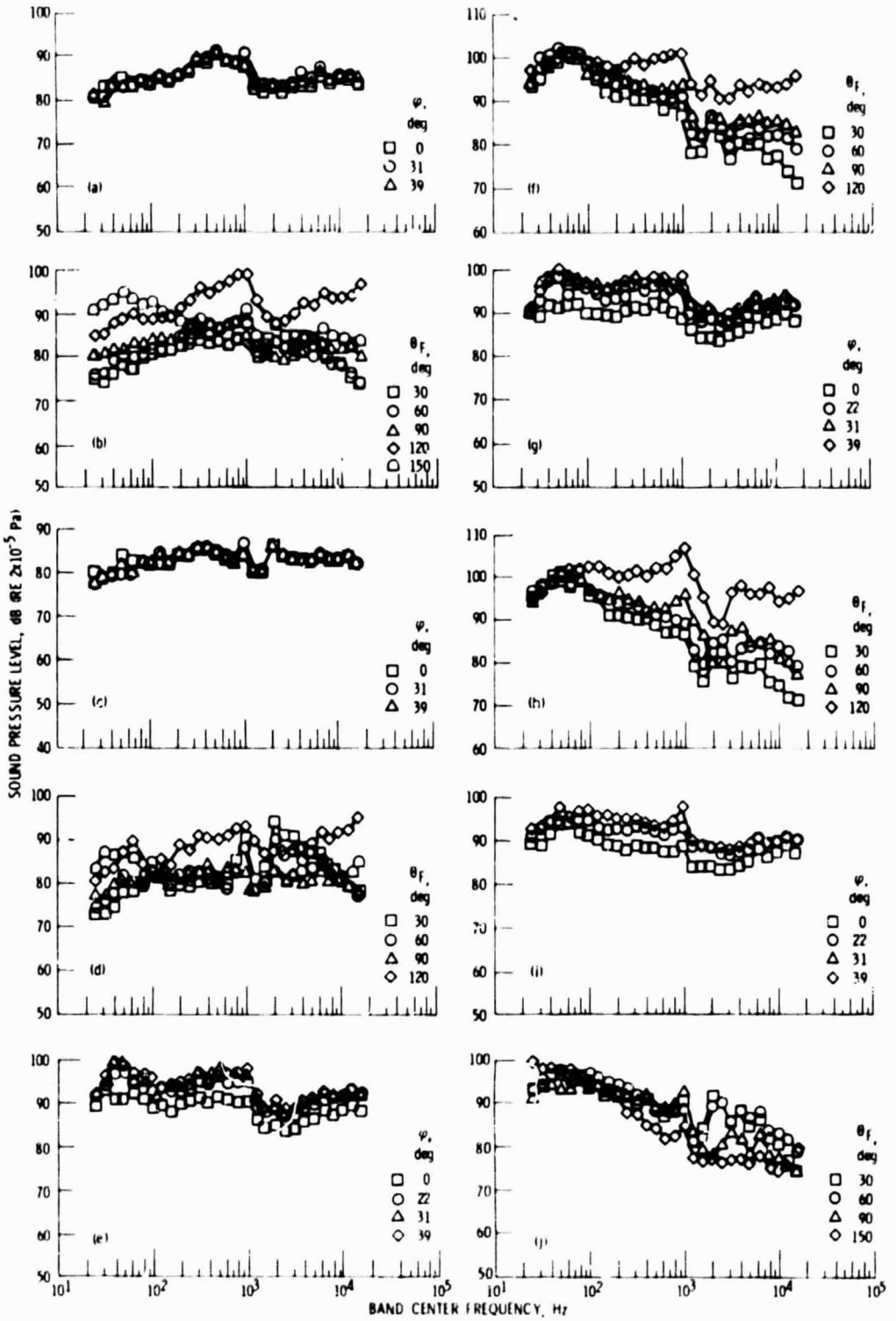


(a) Engine alone; takeoff power; sideline-plane microphones.
(b) Engine alone; takeoff power; flyover-plane microphones.
(c) Engine alone; approach power; sideline-plane microphones.
(d) Engine alone; approach power; flyover-plane microphones.
(e) Engine with wing and 20° flaps; takeoff power; sideline-plane microphones.
(f) Engine with wing and 20° flaps; takeoff power; flyover-plane microphones.
(g) Engine with wing and 30° flaps; takeoff power; sideline-plane microphones.
(h) Engine with wing and 30° flaps; takeoff power; flyover-plane microphones.
(i) Engine with wing and 60° flaps; approach power; sideline-plane microphones.
(j) Engine with wing and 60° flaps; approach power; flyover-plane microphones.

Figure 12. - 1/3-Octave-band spectra. Lossless data at 30.5 m (100-ft) radius.